ELSEVIER

Journal of Alloys and Compounds 311 (2000) 299–304

Journal of ALLOYS AND COMPOUNDS

www.elsevier.com/locate/jallcom

Investigations of the corrosion behaviour of nanocrystalline Nd–Fe–B hot pressed magnets

A.M. El-Aziz, A. Kirchner, O. Gutfleisch, A. Gebert*, L. Schultz

Institute for Solid State and Materials Research Dresden, P.O. Box 270016, D-01171 Dresden, Germany

Received 9 June 2000; accepted 26 June 2000

Abstract

The corrosion behaviour of Nd–Fe–B nanocrystalline magnets made from differently processed powders such as melt spun, intensively milled and HDDR (Hydrogenation–Disproportionation–Desorption–Recombination) powders has been investigated in sulphuric acid solution and in air at 25°C. It is observed that the corrosion resistance of the investigated magnets can be correlated with the grain size of the hardmagnetic phase and the distribution and composition of the Nd-rich intergranular phases. The magnet made from HDDR powder exhibits a comparable, if not better, corrosion resistance in acid solution than magnets made from melt spun and intensively milled powders. Small additions of Co, Al and Ga improved the corrosion resistance of the investigated magnets by replacing the high corrosion sensitive intergranular Nd-rich phases with more noble phases. The surface layer formed during anodic polarization of the HDDR magnet was analysed by Auger electron spectroscopy indicating the formation of (Nd,Fe)-oxide with small amounts of Co and Al. The measured electrostatic surface potential differences of magnets containing Co, Al and Ga were lower than those of magnets without alloying additives.

Keywords: Corrosion; Nd–Fe–B nanocrystalline magnets; Alloying elements; Electrostatic surface potential

1. Introduction

Nd–Fe–B-based permanent magnets exhibit excellent magnetic properties, but they suffer strongly from corrosion in many aggressive environments, such as acidic and salt solutions at ambient temperature and humid air [1,2]. The low corrosion resistance of Nd–Fe–B-based magnets is attributed mainly to the presence of multiple phases in their microstructure and the large electrochemical potential differences between them [3], resulting in the preferential dissolution of the Nd-rich and B-rich intergranular phases and subsequent breaking off of the ferromagnetic grains [4,5]. The detrimental effect of hydrogen in the corrosion process of Nd–Fe–B magnets has been discussed, i.e. the reactivity of these alloys with hydrogen and its easy absorption, which makes the application of a cathodic protection impossible [6,7]. The effect of alloying additions on magnetic properties and corrosion behaviour has been the subject of many investigations. Improved corrosion resistance of sintered Nd–Fe–B-based magnets is achieved by small additions of alloying elements such as Al, Co and Cr [8–11]. According to Fidler [12] there are two types of dopant elements: Type M_1=(Al, Cu, Zn, Ga, Ge, Sn) and M_2=(V, Mo, W, Nb, Ti, Zr); the former forming Nd–M_1 or Nd–Fe–M_1 intergranular phases, the latter forming M_2–B or Fe–M_2–B intergranular phases. Because of their more positive corrosion potentials compared to those of additive-free phases, the new phases which are formed at grain boundaries inhibit dissolution of intergranular regions. However, these alloy modifications improve the corrosion resistance only to a certain degree. Presently, various attempts are directed to optimise the various preparation techniques, such as the powder metallurgical sintering process [13] leading to microcrystalline materials and the melt spinning route [14], the intensive milling process [15,16] and HDDR (Hydrogenation–Disproportionation–Desorption–Recombination) leading to nanocrystalline materials [17,18]. The nanoscale powders are of growing importance, especially for the production of bonded and fully dense hot pressed magnets. These magnets have different corrosion behaviour compared to sintered magnets resulting from the differences in their microstructure, i.e. grain sizes and phase distributions.

In the present work the corrosion behaviour of the hot

---

*Corresponding author.

E-mail address: gebert@ifw-dresden.de (A. Gebert).

0925-8388/00/$ – see front matter
PII: S0925-8388(00)01112-9

pressed nanocrystalline Nd–Fe–B magnets prepared by HDDR processing, melt spinning and intensive milling as well as the effect of alloying additions such as Co, Al and Ga have been investigated in acid solution.

2. Experimental

Fully dense, magnetically isotropic, Nd–Fe–B magnets partly with small additions were prepared by hot pressing of powders obtained by different processing routes: intensive milling, melt spinning and HDDR. The preparation parameters are described elsewhere [19]. The chemical compositions of the investigated materials are listed in Table 1. The magnets were cut with a diamond disc into specimens with surface areas of 0.1 cm^2 for electrochemical tests and 1 cm^2 for gravimetric tests.

The microstructure of the hot pressed magnets was characterized by means of scanning electron microscopy (SEM) using the backscattered electron mode (BSE) and after etching the surface (N_2-purged 0.1 M H_2SO_4 solution for 60 s) using the secondary electron mode (SE). Chemical analysis of the different phases was performed by energy dispersive X-ray (EDX) analysis.

Electrostatic surface potential differences between the ferromagnetic phase and intergranular regions were measured in air at 25°C by means of scanning probe microscopy (Nanoscope III/SPM) [5].

In order to characterize the corrosion behaviour, the following investigations were carried out:

1. Gravimetric measurements. Spontaneous dissolution in free corroding conditions in N_2-purged 0.5 M H_2SO_4, $T=25$°C.
2. Electrochemical measurements. Potentiodynamic polarization tests in N_2-purged 0.5 M H_2SO_4 were carried out using a platinum net as the counter electrode and a saturated calomel electrode as the reference electrode at a disc rotation rate of 720 rpm and a potential scanning rate of 2 mV s^{-1}. Surface layers formed during anodic polarization of the samples were analysed by Auger electron spectroscopy (AES).

3. Results and discussion

3.1. Microstructural investigations

The SEM micrographs (backscattered mode) of the Nd–Fe–B nanocrystalline magnets (without additives) are shown in Fig. 1(a). The regions with white contrast were identified by EDX analysis as the Nd-rich phase and the grey regions represent the ferromagnetic phase. The black areas are holes, which appear during surface finishing. The microstructures of the different types of magnets reveal significant differences especially with respect to the distribution of intergranular phases. The Nd-rich phase appears predominantly as thin white contrast along the ribbon interfaces in the magnet made from melt spun powder (micrograph M1). In the magnet made from intensively milled powder (micrograph I1) the Nd-rich phase is inhomogeneously distributed between powder particles of the ferromagnetic phase, this is similar to the magnet made from HDDR processed material (micrograph H1). The SEM micrographs (SE mode) after etching the samples surface are represented in Fig. 1(b). The average size of ferromagnetic grains of the magnet H1 is in the range of 300 nm, in the case of the magnets M1 and I1 it is in the range 20–100 nm. The EDX analysis of the HDDR H2, melt spun M2 and intensively milled I2 containing Co, Al, Ga suggests the formation of $Nd(Fe,Co)_2$ instead of the common Nd-rich phase in the intergranular regions, especially for the magnet H2. The formation of this phase was also found in sintered magnets by Bala et al. [10] and Mello et al. [20]. While in the case of the magnets M2 and I2, the ordinary Nd-rich phase was found containing cobalt by a given formula of $Nd_4(Fe,Co)$. On the other hand, Al and Ga could not be detected by EDX measurements because of their lower concentration in the samples. Generally, the solubility of Al in the ferromagnetic phase is higher than in the Nd-rich phase and Ga is reported to have a very low solubility in the ferromagnetic phase [21].

3.2. Corrosion behaviour

Corrosion rates determined from weight loss measurements in acid solution of the nanocrystalline Nd–Fe–B

Table 1
Chemical composition (ICP-spectrometry) of the tested materials

Sample	Element (at.%)							Prepared by
	Nd	Dy	Fe	B	Co	Al	Ga	
H1	15.38	–	77.85	6.77	–	–	–	HDDR
H2	13.9	–	62.3	6.8	16.2	0.5	0.3	HDDR
H3	15	1.5	76.9	6	–	–	0.6	HDDR
M1	14	–	80	6	–	–	–	Melt spinning
M2	13.6	–	73.6	5.6	6.6	–	0.6	Melt spinning
I1	16.2	–	78.2	5.6	–	–	–	Intensive milling
I2	13.9	–	62.3	6.8	16.2	0.5	0.3	Intensive milling

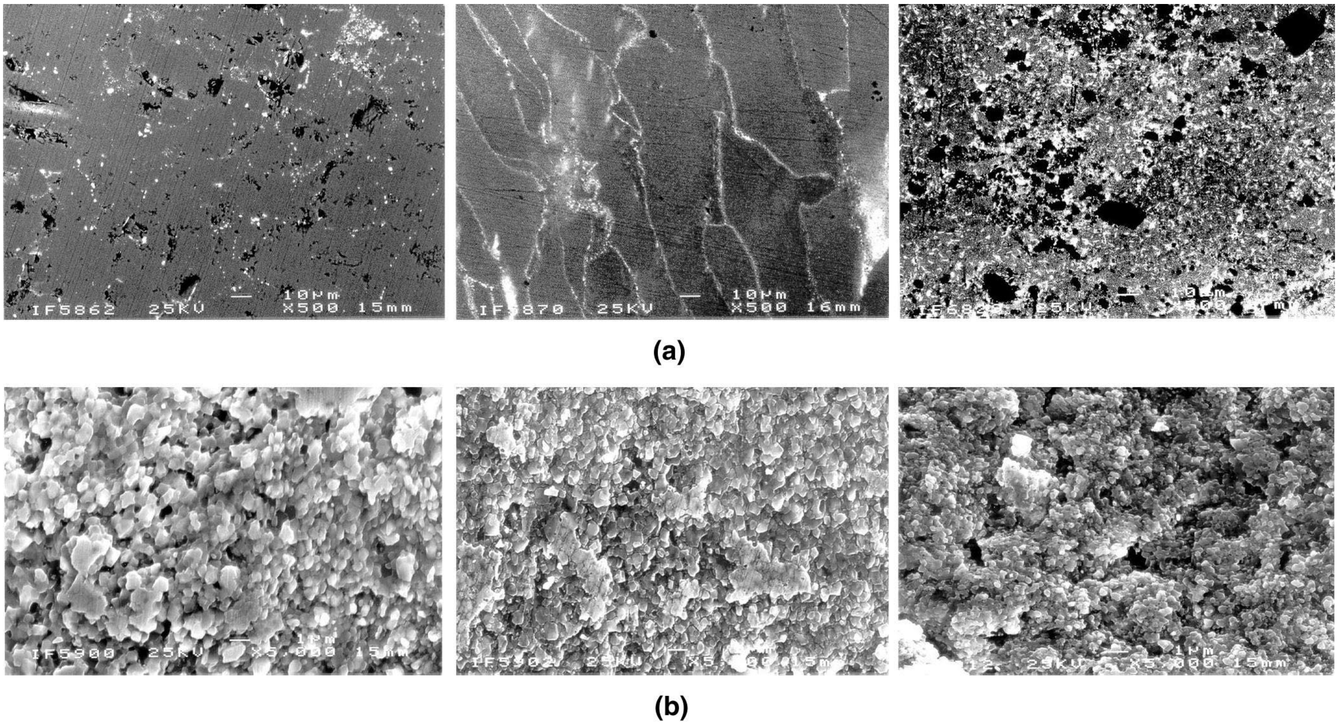

Fig. 1. (a) SEM micrographs (backscattering mode) of nanocrystalline Nd–Fe–B magnets. From left to right: H1, HDDR material; M1, melt spun material; I1, intensively milled material. (b) SEM micrographs (SE mode) of nanocrystalline Nd–Fe–B magnets after etching the surface in N_2-purged 0.1 M H_2SO_4 for 60 s. From left to right: H1, HDDR material; M1, melt spun material; I1, intensively milled material.

magnets made from HDDR, melt spun and intensively milled powder (with and without additions) are represented in Fig. 2. For the HDDR H1 magnet (without alloying additions) immediately after the immersion, the corrosion rate is comparatively low with a value of 60 mg cm^{-2} h, while in the case of melt spun M1 and intensively milled I1 magnets the initial values are 120 and 200 mg cm^{-2} h, respectively. Then for all the samples the corrosion rate increases rapidly resulting from the partial dissolution of Nd-rich intergranular region as well as the falling out of

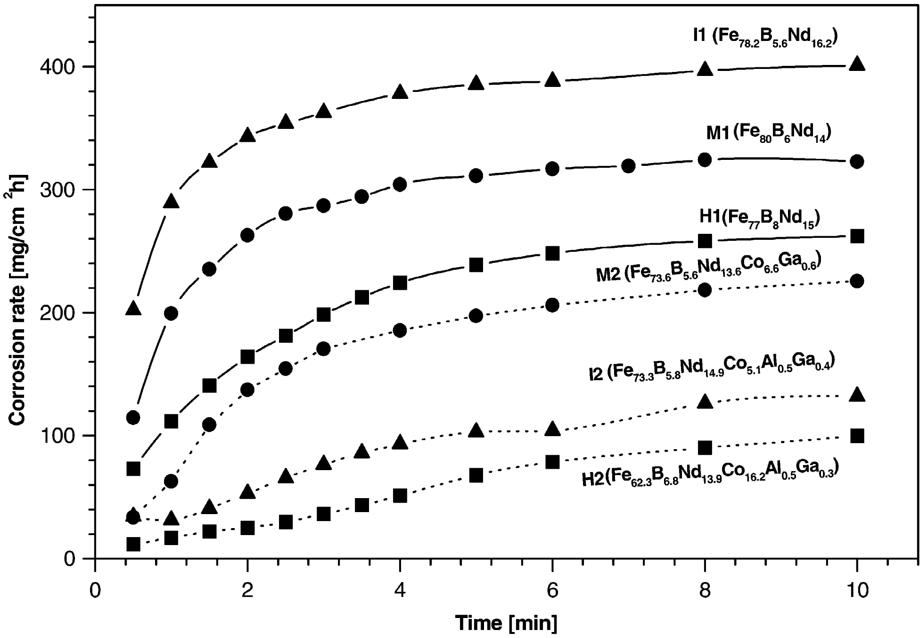

Fig. 2. Corrosion rates of HDDR, melt spun and intensively milled magnets in N_2-purged 0.5 M H_2SO_4 at 25°C.

the ferromagnetic grains. After about 5 min of immersion relative steady-state values are reached and after 10 min the corrosion rate for these ternary nanocrystalline magnets decreases in the following order:

Intensively milled I1 magnet $>$ melt spun M1 magnet
$>$ HDDR H1 magnet

The above observation suggests that the corrosion resistance of the nanocrystalline magnets increases with increasing grain size of the ferromagnetic phase. This may result from a smaller fraction of grain boundaries in the microstructure of the magnets with larger grain size [22]. As observed from microstructural investigations [Fig. 1(b)], the magnet HDDR H1 has a larger average grain size than the magnets melt spun M1 and intensively milled I1, respectively. However, a more detailed study of the distribution of the intergranular phases, which also affects the corrosion behaviour, is necessary to fully understand these observations.

As shown in Fig. 2 the acid corrosion rates are significantly lower for the magnets HDDR H2, melt spun M2 and intensively milled I2 (with additions of Co, Al and Ga). With respect to the literature data [5] and our EDX investigations, this is attributed mainly to the replacement of the low corrosion resistant Nd-rich intergranular phase by higher corrosion resistant Nd-based phases containing Co and Al. The magnet H2 made from HDDR processed powder with Co, Al and Ga additives ($Nd_{13.9}Fe_{62.3}Co_{16.2}Al_{0.5}Ga_{0.3}B_{6.8}$) shows the highest corrosion resistance under these experimental conditions. In order to study the effect of the different additives, similar corrosion tests were performed on magnets prepared from various HDDR processed powders and the results are shown in Fig. 3. The corrosion rate of the magnet H3 (with Dy and Ga) is lower than that of the magnet H1 (without additions), despite the higher rare earth content of the magnet H3 (16.5 at.%) compared to that of magnet H1 (15.3 at.%). The combined addition of Dy and Ga decreases the corrosion rate of the magnet H3. On the other hand, the low rare earth content of the magnet H2 (13.9 at.%) and the addition of 16 at.% Co improve the corrosion resistance distinctly.

The electrostatic surface potential differences between the ferromagnetic phase and intergranular regions of the investigated magnets were measured. As reported by Schultz et al. [23,5], the higher the electrostatic surface potential difference the higher is the corrosion rate of sintered magnets. The measured electrostatic surface potentials of the magnets H2, M2 and I2 containing Co, Al and Ga are lower than those of the magnets H1, M1 and I1 (without alloying additives). This result reflects the high stability of the intergranular regions containing Co, Al and Ga of the magnets H2, M2 and I2.

The potentiodynamic polarization curves of the HDDR H1, melt spun M1 and intensively milled I1 powder magnets measured in acid solution are represented in Fig. 4. For comparison, a HDDR H2 magnet (with Co, Ga and Al alloying additives) is also shown. In contrast to the results of gravimetric tests, there is no significant correlation with respect to the powder processing routes. The corrosion current densities of the magnets made from HDDR H1, melt spun M1 and intensively milled I1 powder were calculated showing a value of 30 mA cm^{-2} for magnet H1 and 6 and 8 mA cm^{-2} for magnets M1 and I1, respectively. This indicates a slightly higher corrosion

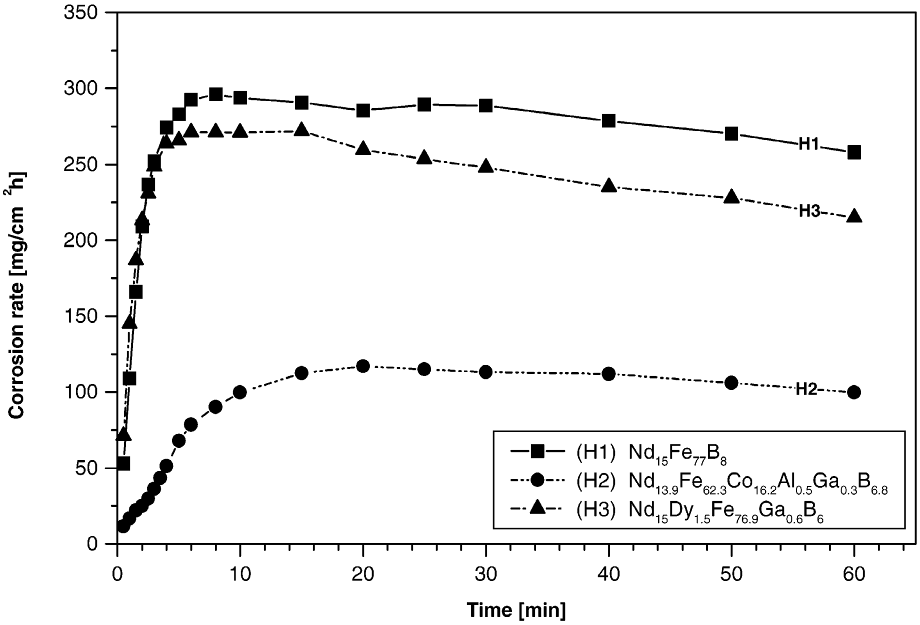

Fig. 3. Corrosion rates of HDDR magnets containing different alloying additives in N_2-purged 0.5 M H_2SO_4 at 25°C.

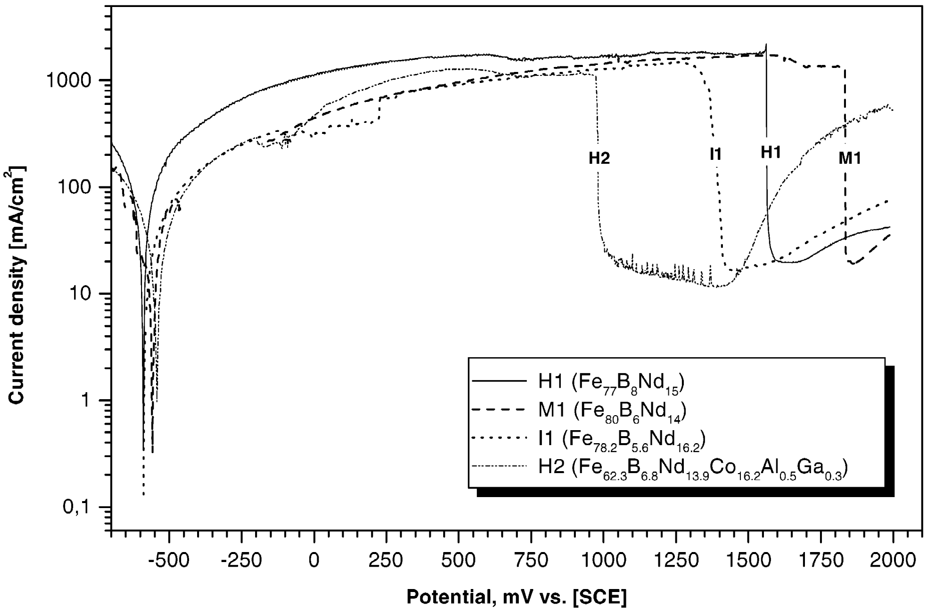

Fig. 4. Potentiodynamic polarization curves of magnets made from HDDR, melt spun and intensively milled powders in N_2-purged 0.5 M H_2SO_4 at 720 rpm, 2 mV s^{-1}, 25°C.

rate for the magnet made from HDDR processed powder under the present conditions compared to the other magnets. This significant difference in the corrosion rates obtained from gravimetric and electrochemical measurements for the different processed materials is not clearly understood, yet. However, one must consider the main difference in the testing procedures: weight loss mainly refers to solid corrosion products (ferromagnetic grains), whereas the corrosion current densities are related to charge transfer reactions at the surface, i.e. metal dissolution and hydrogen reduction (mainly intergranular phases). At very high anodic potentials, above 1.4 V, the magnets H1, M1 and I1 show a ‘quasi-passive’ state indicating a relatively low protective effect of the surface layers formed. The polarization curve measured for the magnet H2 indicates a significant effect of the alloying elements on the anodic polarization behaviour. The corrosion current density is about 3 mA cm^{-2}, which is significantly lower compared to that of the magnet H1 (without alloying additives) and the ‘quasi-passive’ state appears at a potential higher than 900 mV and extends over a broader potential range indicative of the protective effect of the formed surface layers. The film formed in the ‘quasi-passive’ region of the magnet H2 was analysed by Auger Electron Spectroscopy (AES) showing (Nd,Fe)-oxide with a low concentration of Co and Al alloying elements.

The corrosion inhibition of the magnet HDDR H2 by Co, Al and Ga compared to the magnet H1 (without alloying additives) results mainly from the change in the microstructure by segregation of these kinds of additions into intergranular regions. This process leads to a decrease of the electrochemical potential difference between the ferromagnetic phase and the intergranular regions [10,24].

4. Conclusions

The corrosion behaviour of different nanocrystalline Nd–Fe–B magnets with and without the addition of Co, Al and Ga has been determined using gravimetric and electrochemical techniques, accompanied by SEM, SPM and AES investigations. Based on the results obtained from our present investigation, the following conclusions can be drawn:

1. The process of preparation of the magnets has a significant influence on the corrosion behaviour. The magnets made from HDDR powder are in terms of their corrosion resistance comparable, if not better, to the magnets made from melt spun and the intensively milled powders.
2. The Co, Al and Ga additions to the magnet powder reduce the rate of dissolution in acid solution and improve the corrosion resistance by increasing the stability of the Nd-rich phase. In addition, the magnet made from HDDR processed powder with Co, Al and Ga additives made from HDDR processed powder is in this study more corrosion resistant than those made of melt spun and intensively milled powders under the same experimental conditions.

Acknowledgements

The authors acknowledge helpful discussions with K. Mummert. The authors would like to thank G. Barkleit, A. Güth and A. John for carrying out SPM, SEM and AES investigations and V. Panchanathan for supplying the melt spun powders.

References

[1] D.F. Cygan, M.J. McNallan, J. Magn. Mater. 139 (1995) 131.
[2] C.J. Willman, K.V.L. Narasimhan, J. Appl. Phys. 61 (1987) 3766.
[3] I. Costa, I.J. Sayeg, R.N. Faria, in: Proc. 14th Inter. Workshop Rare-Earth Magnets and Their Applications, Sao Paulo, Brazil, Vol. 1, 1996, p. 264.
[4] O.B.G. Assis, V. Sinka, M. Ferrante, I.L. Oliveira, J. Alloys Comp. 218 (1995) 263.
[5] K. Mummert, A.M. El-Aziz, G. Barkleit, W. Rodewald, L. Schultz, Mater. Corr. 51 (2000) 13.
[6] H. Bala, S. Szymura, Corros. Sci. 32 (1991) 953.
[7] G. Yan, A.J. Williams, J.P.G. Farr, I.R. Harris, J. Alloys Comp. 292 (1999) 266.
[8] H. Bala, S. Szymura, E. Owczarek, W. Nowy-Wiechula, Intermetallics 5 (1997) 493.
[9] K. Ohashi, Y. Tawara, T. Yokoyama, N. Kobayashi, in: C. Herget, R. Poerschke (Eds.), Proc. Inter. Workshop on Rare Earth Magnets and Their Applications, Bad Soden, Germany, Deutsche Physikalische, Bad Honnef, 1987, p. 355.
[10] S. Szymura, H. Bala, G. Pawlowska, J. Less-Common Met. 175 (1991) 185.
[11] H. Bala, G. Pawlowska, S. Szymura, V.V. Sergeev, Yu.M. Rabinovich, J. Magn. Magn. Mater. 87 (1990) L255.
[12] J. Fidler, in: Proc. 7th Inter. Symp. on Magnetic Anisotropy and Coercivity in Rare-Earth Transition Metal Alloys, Canberra, Australia, 1992, p. 11.
[13] M. Sagawa, S. Fujimura, N. Togawa, N. Yamamoto, Y. Matsuura, J. Appl. Phys. 55 (1984) 2083.
[14] J.J. Croat, J.F. Herbst, R.W. Lee, F.E. Pinkerton, J. Appl. Phys. 55 (1984) 2078.
[15] L. Schultz, J. Wecker, E. Hellstern, J. Appl. Phys. 61 (1987) 3583.
[16] L. Schultz, Mater. Sci. Forum 88–90 (1990) 687.
[17] T. Takashita, R. Nakayama, in: Proc. 10th Inter. Workshop on Rare Earth Magnets and Their Applications, Kyoto, Japan, 1989, p. 551.
[18] O. Gutfleisch, I.R. Harris, J. Phys. D: Appl. Phys. 29 (1996) 2255.
[19] A. Kirchner, W. Grünberger, O. Gutfleisch, V. Neu, K.-H. Müller, L. Schultz, J. Appl. Phys. 31 (1998) 1660.
[20] M. Mello, O.B.G. Assis, M. Ferrante, V. Sinka, in: Proc. 14th Inter. Rare Earth Magnets and Their Applications, Sao Paulo, Brazil, Vol. 1, 1996, p. 417.
[21] B. Grieb, C. Pithan, E.-Th. Henig, G. Petzow, J. Appl. Phys. 70 (1991) 6354.
[22] S. Szymura, H. Bala, Yu.M. Rabinovich, V.V. Sergeev, G. Pawlowska, D.V. Pokrovskii, J. Phys.: Condens. Mater. 3 (1991) 5893.
[23] L. Schultz, A.M. El-Aziz, G. Barkleit, K. Mummert, Mater. Sci. Eng. A267 (1999) 307.
[24] A.M. El-Aziz, G. Barkleit, M. Herrich, K. Mummert, L. Schultz, B. Grieb, in: Proc. 15th Inter. Workshop on Rare Earth Magnets and Their Applications, Dresden, Germany, Vol. 1, 1998, p. 905.